

# Chemoenzymatic Synthesis of Plant-Derived Kavalactone Natural Products by Dynamic Resolution Using a Biosynthetic O-Methyltransferase Tailoring Enzyme

Simon Rydzek,<sup>[a]</sup> Florian Guth,<sup>[a]</sup> Steffen Friedrich,<sup>[a]</sup> Jakob Noske,<sup>[b]</sup> Birte Höcker,<sup>[b]</sup> and Frank Hahn<sup>\*[a]</sup>

Biosynthetic enzymes have enormous potential for the chemoenzymatic synthesis of natural products and other bioactive compounds. Methyltransferases are promising tools for the selective enzymatic modification of complex structures. This paper describes the production, purification and biochemical characterization of the O-methyltransferase JerF, which catalyzes unique 4-methoxy-5,6-dihydropyranone formation in jergolid A biosynthesis. Isolation problems had hitherto prevented detailed studies on JerF and were solved by the fusion to maltose-binding protein. The differentiation of JerF between styryl-substituted dihydropyranidion enantiomers was investigated. In combination with a spontaneous racemization occurring with this type of substrates, a new enzymatic dynamic

kinetic resolution was observed, which was used for the enantioselective chemoenzymatic synthesis of kavalactone natural products and new derivatives. In combination with an HMT-based SAM regeneration system, (+)-kavain, (+)-11,12-dimethoxykavain and (+)-12-fluorokavain were prepared in 3–4 steps on a 100  $\mu\text{mol}$  scale with overall yields of 37–57% and *ees* of 70–86%. A mutational study based on an AlphaFold 2 model provided indications for active site residues with an influence on the performance of the enzyme that could be targeted for engineering in the future. This example illustrates how the exceptional enzymatic activities and specificities of biosynthetic enzymes can be exploited for the development of new synthesis approaches.

## Introduction

The biosynthetic pathways of natural products are a virtually inexhaustible source of novel enzymes with potential for use in biocatalysis and chemoenzymatic synthesis.<sup>[1]</sup> Compared to enzymes of the primary metabolism, biosynthetic enzymes are characterized by a greater diversity of enzymatic activities.<sup>[2]</sup> Enzymes from the late stages of biosynthetic pathways act on complex scaffolds and often exhibit interesting selectivity that can be exploited in the chemoenzymatic synthesis of complex molecules.

S-adenosyl methionine (SAM)-dependent enzymes are among nature's most versatile enzymes and are involved in such different processes as natural product biosynthesis or epigenetic DNA methylation.<sup>[3]</sup> SAM-dependent methyltransferases (MTs) catalyze the transfer of electrophilic methyl

groups from SAM to C, O, N or S nucleophiles and participate in the assembly of all natural product classes.<sup>[4,5]</sup> Methylation is also important for research fields like medicinal chemistry where the magic methyl effect is used to optimize the biological activity of drugs.<sup>[6]</sup> The use of MTs for late-stage modification and diversification is therefore a promising emerging tool for natural product and drug synthesis.<sup>[7]</sup>

Significant progress has recently been made regarding the applicability and scope of MT biocatalysis.<sup>[8–11]</sup> It has been shown that MTs can accept SAM derivatives such as S-adenosyl ethionine (SAE), opening the possibility to introduce other alkyl residues than methyls.<sup>[12]</sup> In situ formation of SAM (analogues) by methionine adenosyltransferases (MATs) and hydrolysis of inhibitory S-adenosyl homocysteine (SAH) by SAH hydrolases or methylthioadenosine nucleosidases (MTANs) can be coupled to MT reactions.<sup>[12–14]</sup> SAM can also be directly regenerated from SAH in situ by halide methyltransferases (HMTs) or complex cascades of SAH hydrolases, polyphosphate kinases and MATs, thus shifting the stoichiometric agent from SAM towards available electrophilic alkylating agents such as methyl iodide or methionine and polyphosphate, respectively.<sup>[11,15,16]</sup> Advances in protein engineering have also made it possible to tailor MT selectivity, for example to target specific nucleophilic positions in drug-like heterocycles.<sup>[17,18]</sup> To realize the potential of biosynthetic methyltransferases in the chemoenzymatic synthesis of natural products and other chiral molecules, it is necessary to integrate them into new synthetic approaches that exploit their specific selectivity advantages.

[a] S. Rydzek, F. Guth, S. Friedrich, F. Hahn  
Department of Chemistry, Faculty of Biology, Chemistry and Earth Sciences,  
University of Bayreuth, Universitätsstraße 30, Bayreuth 95447, Germany  
E-mail: frank.hahn@uni-bayreuth.de

[b] J. Noske, B. Höcker  
Department of Biochemistry, University of Bayreuth, Universitätsstraße 30,  
Bayreuth 95447, Germany

Supporting information for this article is available on the WWW under  
<https://doi.org/10.1002/cctc.202400883> Supporting information for this article is available on the WWW under <https://doi.org/10.1002/cctc.202400883>

© 2024 The Authors. ChemCatChem published by Wiley-VCH GmbH. This is an open access article under the terms of the Creative Commons Attribution License, which permits use, distribution and reproduction in any medium, provided the original work is properly cited.

The jerangolids are polyketide natural products produced by *Sorrangium cellulosum* So ce307 and, like the structurally and biosynthetically closely related ambruticins, are under scrutiny for their antifungal activity (Figure 1A).<sup>[19–21]</sup> The O-methyltransferase JerF acts as a tailoring enzyme in jerangolid A (3) biosynthesis and transforms the polyketide synthase product projerangolid (1) into the intermediate jerangolid E (2).<sup>[22–24]</sup> The methyleneoether introduced by JerF is an

essential structural motif that enables RIESKE oxygenase-catalyzed oxidations into jerangolid A (3). O-methylation of aromatic hydroxypyranones is a common biosynthetic event.<sup>[25–27]</sup> The methylation of the non-aromatic, chiral 5,6-dihydro-2H-pyran-2,4-dione motif is however rare and no other enzyme catalyzing this step has been characterized to date.<sup>[23,24]</sup> In bioconversion experiments in which dihydropyranone precursors were fed to *E. coli* cells expressing the *jerF* gene, we found highly regioselective 4-O-methylation and tolerance for a diverse variety of residues in the positions highlighted with R<sup>1</sup> and R<sup>2</sup> in Figure 1B. Interestingly, we observed a considerable enantiomeric excess in the products of the reaction with the racemic substrate bearing R<sup>1</sup> = H and R<sup>2</sup> = Ph. This points towards a discrimination between the precursor enantiomers by JerF that might be of synthetic value in the synthesis of (+)-kavain ((R)-7a) and other (+)-kavalactones bearing the 4-methoxy-5,6-dihydro-2H-pyran-2-one motif (e.g. (R)-8, (R)-10 and (R)-11 in Figure 2A).

Kavalactones are plant natural products with pharmacological relevance.<sup>[28,29]</sup> 20 different kavalactones have been isolated from kava plant extracts of which 96% are represented by the compounds depicted in Figure 2A.<sup>[30]</sup> Racemic and enantioselective syntheses of kavalactones containing a methoxy-5,6-dihydro-2H-pyran-2-one have been published (Figure 2B).<sup>[28,31–36]</sup> The key transformations in these were either cross-coupling reactions between the vinyl dihydropyranone *rac*-14 and aryls (15)<sup>[31–34]</sup> or (vinylogous) aldol reactions of cinnamaldehydes (16) followed by lactonization, respectively, followed by regioselective O-methylation using Me<sub>2</sub>SO<sub>4</sub>.<sup>[28,31,35]</sup>

We wanted to isolate and further biochemically characterize JerF to better understand the relevant properties for a synthetic application and to enable specific optimization of its use. The application should be a chemoenzymatic synthesis of kavalactones for which JerF is particularly suited as its use could lead to a conceptually new synthetic approach based on late-stage enzymatic O-methylation-kinetic resolution. This would eliminate the need for stereoselective organic transformations in kavalactone synthesis that require transition metals and chiral auxiliaries. The relaxed substrate specificity of JerF also promises that it could be suitable for the synthesis of a wide range of derivatives.

## Results and Discussion

### Enzyme Characterization and Reaction Setup

In our previous studies on JerF, we observed that isolation of JerF (fusion proteins) in soluble and active form was not successful with various tested expression systems.<sup>[22–24]</sup> We attempted the production of non-tagged as well as His<sub>6</sub> and GST-tagged JerF from (cold shock) expression of the sequence-optimized *jerF* gene in the *pET28a(+)*, *pET20b(+)*, *pCOLDI* and *pGEX* plasmids. We therefore conducted bioconversion experiments using the cell-free lysate of the *his<sub>6</sub>-jerF* expression in *E. coli* instead. A fast and virtually complete

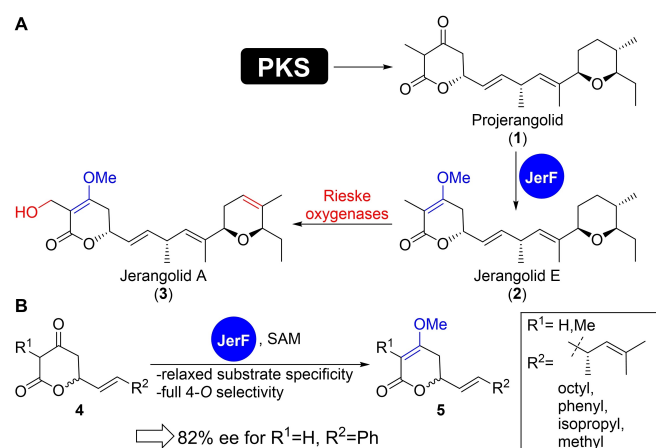


**Figure 1.** A: The O-methyltransferase JerF catalyzes formation of a methyleneoether in the biosynthesis of jerangolid A (3). B: Bioconversion of diverse projerangolid derivatives (4) by *jerF-E. coli*. PKS: polyketide synthase.<sup>[22–24]</sup>

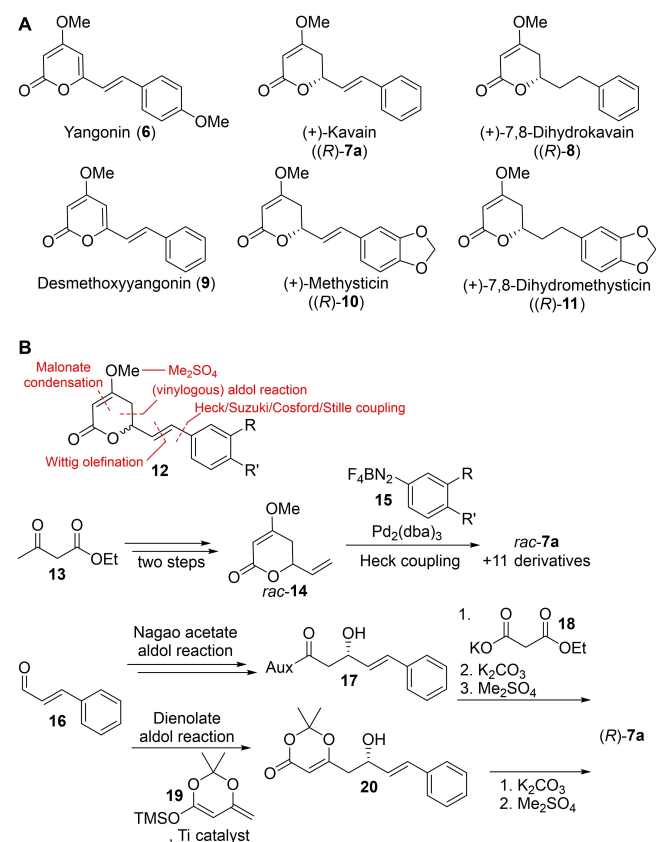


**Figure 2.** A: Main components in kava plant extracts. B: Key bond formations in previous kavalactone syntheses and representative routes to *rac*-7a and (R)-7a.<sup>[31,33]</sup>

conversion of the natural precursor **1** occurred within 1 h under these conditions. This system was however not suitable for a further characterization of JerF so that we now aimed to obtain purified protein.

In this study, we attempted to produce His<sub>6</sub>-tagged JerF fusion proteins based on existing expression constructs in *E. coli* BL21 derivatives such as BL21 Star, C41, Tuner and SoluBL, which are designed to facilitate soluble production (Figure S61). In no case sufficient amounts of soluble protein were obtained. Denaturation followed by refolding of His<sub>6</sub>-JerF by dialysis in the presence of arginine yielded a soluble protein that could be brought to good purity by affinity chromatography (Figure S62). Unfortunately, this preparation showed no activity in test reactions, so that we decided to proceed with a fusion protein with a strongly solubility-promoting tag.

The *jerF* gene was cloned into the pETMBP-1a vector and expressed in *E. coli* BL21, giving the soluble maltose-binding protein (MBP)-JerF fusion protein that could be purified by MBP affinity chromatography (Figure S59). Cleavage of the MBP-tag via Tobacco Etch Virus (TEV)-protease was only partially successful and efforts to isolate the tag-free protein by reverse affinity chromatography again led to insoluble JerF. Purified MBP-JerF was therefore used in the subsequent

*in vitro* assays. Enzymatic activity was observed in the reaction with the (±)-kavain precursor *rac*-**21 a**, giving 35% conversion after 8 h (Figure 3A, Figure S73). This value was between those obtained for the corresponding reactions with the lysates of *his6-jerF* (24%) and *mbp-jerF* (55%) expressions in *E. coli* (normalized to the same amount of cells before cell disruption). SDS-PAGE analysis showed that the ratio of JerF fusion protein in the soluble fraction was considerably higher for the MBP-tagged construct (Figure S59).

An analysis of the kinetic parameters for JerF was performed using a commercially available MTase assay kit (Promega, Figures S63–64). The values observed for the natural JerF precursor projerangolid (**1**) were in a range comparable to those of other MTs ( $k_{\text{cat}} = 0.383 \pm 0.003 \text{ min}^{-1}$ ,  $K_{\text{M}} = 4.01 \pm 0.12 \text{ } \mu\text{M}$ ; Figure 3B).<sup>[37,38]</sup> The corresponding values for the two enantiomers of **21 a** showed an overall significantly slower reaction than with **1** and a preference for (*R*)-**21 a** ( $k_{\text{cat}} = 0.0476 \pm 0.0009 \text{ min}^{-1}$ ,  $K_{\text{M}} = 28.8 \pm 2.5 \text{ } \mu\text{M}$ ) over (*S*)-**21 a** ( $k_{\text{cat}} = 0.0275 \pm 0.0005 \text{ min}^{-1}$ ,  $K_{\text{M}} = 106.1 \text{ } \mu\text{M}$ ). This is consistent with the stereoselectivity observed in our previous experiments with the His<sub>6</sub>-JerF lysate, but the difference of the  $k_{\text{cat}}$  and  $K_{\text{M}}$  values would not explain the high *ee* of 84% that was found in the bioconversions.<sup>[24]</sup> Time course experi-

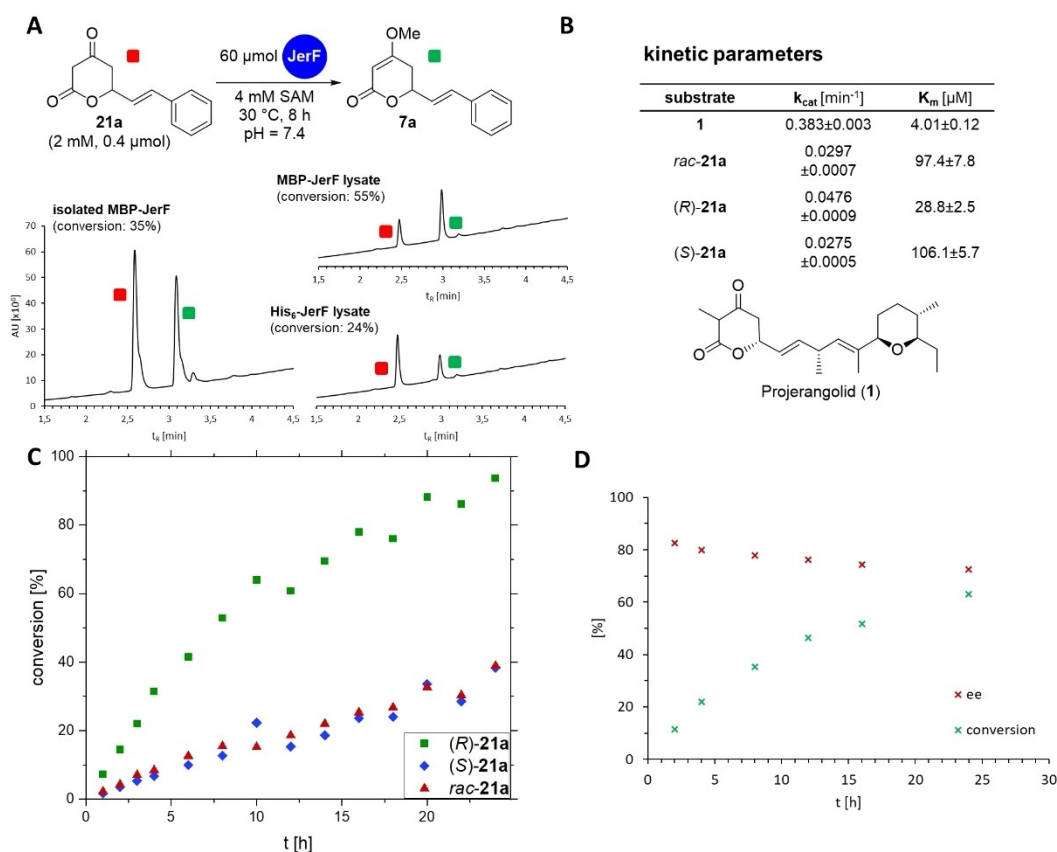
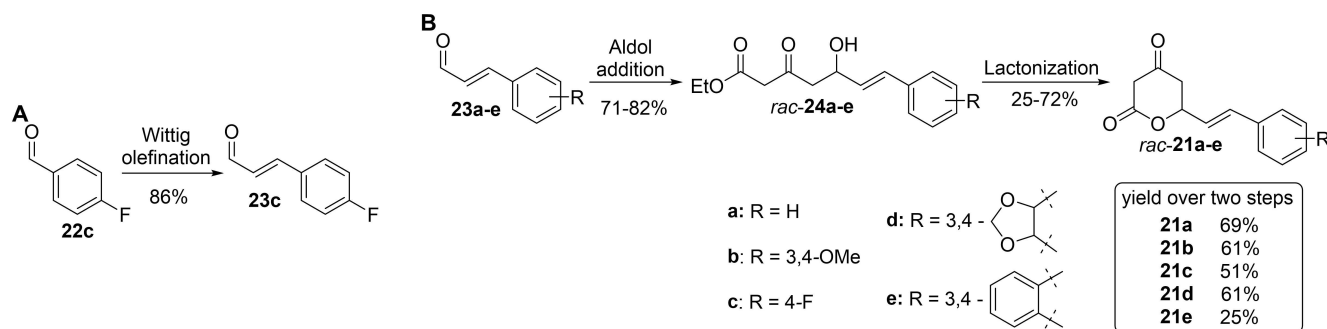


**Figure 3.** Enzymatic conversion of *rac*-**21 a** into kavain (**7 a**). A: comparison of different preparations of JerF from expression in *E. coli*. The conversion was determined from the relative UV peak integrals for substrate and reaction product (Figure S65). B: Summary of the kinetic parameters of MBP-JerF with **1**, *rac*-**21 a**, (*R*)-**21 a** and (*S*)-**21 a**. C: time course for the conversion of (*R*)-**21 a** (green), (*S*)-**21 a** (blue) and *rac*-**21 a** (red) by purified MBP-JerF ( $c = 60 \text{ } \mu\text{M}$ ). Each data point represents a separate reaction stopped after the respective reaction time. The reaction conditions were similar to those in A). D: Course of conversion (red crosses) and *ee* (green crosses) in the reaction of *rac*-**21 a** with MBP-JerF.

ments of MBP-JerF with (*R*)-**21a**, (*S*)-**21a** and *rac*-**21a** were recorded to monitor the progress of the reaction over longer incubation times (Figure 3C, reaction scale  $\sim 0.4 \mu\text{mol}$ ). In line with the previous results, (*R*)-**21a** was converted faster than (*S*)-**21a**. Interestingly, the conversion over time of *rac*-**21a** was very similar to that of (*S*)-**21a**, suggesting interference of both enantiomers of **21a** in binding and conversion by the enzyme or the conversion of both stereoisomers into each other. *rac*-**21a** was incubated with the preparations of JerF described in Figure 3A and conversion and *ee* were monitored over time (Figure 3D). In all cases, the *ee* value was initially high ( $\sim 80\%$ ) and decreased to levels of 70–80% with increasing conversion. The conversion by the lysates went closer to completion than with purified MBP-JerF, pointing towards greater stability of the enzyme in the lysate (Figures S71, S73, S76). Again, the result in the reaction with purified MBP-JerF did not correlate well with the results of the kinetic analysis. Both indicated significantly different *E* values of 6 and  $\sim 19$  for reactions that were carried out under identical conditions (see SI), indicating that an additional process was taking place that improves the stereochemical outcome of the reaction over longer incubation times compared to that suggested by the actual kinetic parameters (see below). Based on the time courses obtained, a duration of 12 h was chosen for the following assays with derivatives of **21a**.

### Substrate Screening and Upscaling

To further investigate the scope of the JerF-catalyzed enantiodiscriminating *O*-methylation for the stereoselective synthesis of (+)-kavalactones, the precursor derivatives *rac*-**21b**–*rac*-**21e** were synthesized in 2–3 steps with overall yields of 25–69% (Scheme 1).<sup>[31,35]</sup> Exemplary time courses that were recorded for the reactions of MBP-JerF with **21b** and **21c** showed similar conversions and *ees* over the time (Figures S73–75) as for **21a**. Endpoint assays of 12 h were performed at a scale of  $2 \mu\text{mol}$  substrate. The precursors *rac*-**21a**–*rac*-**21e** were all accepted by JerF, giving conversions of 22–84% and *ees* of 64–78% (Scheme 2, Table 1, column ' $2 \mu\text{mol}$  scale').



**Scheme 1.** Synthesis of precursor aldehyde **23c** (A) and the racemic kavalactone precursor derivatives **21a–e** used in this study (B). The enantioselective synthesis of reference compounds is reported in the supporting information.



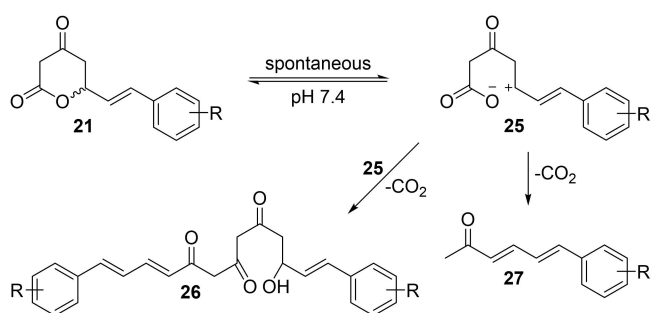
**Scheme 2.** Reaction conditions for enzymatic reactions of substrates **21a–e** with JerF. Results of these reactions are depicted in Table 1.

It is noteworthy that the conversions and *ees* for the reactions of *rac*-**21b** and *rac*-**21d** with JerF (entries 2 and 4) indicate the presence of more than 50% of the respective (*R*)-enantiomers of **7b** and **7d** in the crude product. This again strongly suggests that an additional process that generates (*R*)-**21b** and (*R*)-**21d** from their respective (*S*)-enantiomers takes place in parallel to the enzymatic reaction. To test substrates of type **21** for their propensity to undergo such spontaneous racemization, we incubated the representative compound (*R*)-**21b** in the reaction buffer for 24 h. Racemization into a mixture of (*R*)-**21b** and (*S*)-**21b** was indeed found along with the formation of side products (Figure S127). These compounds could not be isolated, but UPLC-MS and NMR analysis of the crude products of the enzymatic assays and reference incubations provided indications for the formation of decarboxylated compounds of the type **27** and dimers such as **26** (Figures S128 and S129).

We propose a mechanism as shown in Scheme 3 to be responsible for the spontaneous racemization and the formation of the side products. It starts with ring opening of the lactone in **21**, which is assisted by the formation of a highly stabilized styryl cation **25**. This is expected to be particularly pronounced in the case of substituents with a +M-effect on the aryl ring, such as **21b** and **21d**. The ring in **25** can close again to form both enantiomers of **21**, resulting in an overall racemization. From **25**, the methylketone **27** could be formed by decarboxylation. A reasonable path to the dimer **26** leads *via* ring-opening transacylation of a molecule of **21** to the  $\alpha$ -carbon of the vinylmethyl ketone **27** or its enol form. Such spontaneous racemization has previously been exploited for dynamic kinetic resolution processes, for example in the biocatalytic synthesis of  $\beta$ -branched amino acids,<sup>[39]</sup> highlighting the potential of the

entry	precursor	product	2 μmol scale[b]		20 μmol scale[b]		100 μmol scale[c]			100 μmol scale + SAM regeneration[d]			
			conv.	ee	conv.	yield[e]	ee	conv.	yield[e]	ee	conv.	yield[e]	ee
1	<i>rac</i> -21 a	( <i>R</i> )-7 a	46	76	37	35	78	79	70	75	93	82	70
2	<i>rac</i> -21 b	( <i>R</i> )-7 b	78	74	63	47	70	73	68	72	92	84	70
3	<i>rac</i> -21 c	( <i>R</i> )-7 c	51	78	41	40	84	56	49	78	81	73	86
4	<i>rac</i> -21 d	( <i>R</i> )-7 d	81	76	41	40	74						
5	<i>rac</i> -21 e	( <i>R</i> )-7 e	25	64	28	27	67						

<sup>[a]</sup> Conversions and ees were determined from the relative peak integrals in the UPLC-UV/chiral HPLC chromatograms. All data were obtained from single experiments. <sup>[b]</sup> Performed using 60 μM of purified MBP-JerF and 2 mM of the respective substrate. Reaction time: 12 h. <sup>[c]</sup> Performed with cell lysate from MBP-jerF *E. coli* expressions with a total protein concentration of 3 mg/mL. Reaction time: 8 h. <sup>[d]</sup> Reaction conditions as for <sup>[c]</sup> with additional cell lysate from *uma\_E. coli\_Δmtn* expressions (total protein concentration of 1 mg/mL), 5 mM Mel and reduced SAM concentration (20 μM). <sup>[e]</sup> Isolated yields.



**Scheme 3.** Substrates of the type 21 undergo racemization and irreversible degradation under the present reaction conditions (Figures S128 and S129).

combination with stereoselective biocatalysis. Consistent with its nature as a late-stage biosynthetic enzyme that has evolved to act on structurally complex intermediates, JerF allows control of two processes (O-methylation and stereo-differentiation) at different positions of a complex fragment.

No further attempts to optimize the system by varying the pH value were made as previous studies had shown a pH of 7.4 to be optimal for the reaction of JerF with ketolactone substrates like 21. Increased degradation of the ketolactones at pH values  $\geq 8.0$  and a significantly lower activity of JerF at pH values around 7.0 was observed.<sup>[24]</sup> A reasonable way to improve the enantioselectivity of the overall chemoenzymatic dynamic kinetic resolution process would be increasing the (*R*)-selectivity of JerF by protein engineering.<sup>[40]</sup>

Increasing the scale of the enzymatic reaction to 20 μmol of *rac*-21 a–e led to a significant drop in conversion for most of the substrates (Table 1, column '20 μmol scale'). An obvious reason for this was a limited solubility of the substrates in the aqueous environment, which could not be overcome by adding organic co-solvents such as DMSO. Nevertheless, the conversions were in a range that allowed all products to be isolated in sufficient amounts by RP-HPLC for a characterization by NMR. Chiral HPLC analysis showed similar ees as in the experiments on the 2 μmol scale, indicating that the racemization was not compromised by the upscaling.

For further scale-up to 100 μmol of starting material, the reactions were performed with the MBP-JerF-containing cell-

free lysate instead of the purified enzyme. The more complex composition of cell lysates can positively influence the results of reactions with hydrophobic substrates.<sup>[41]</sup> On the one hand, the presence of amphiphilic cellular components can increase the solubility of the substrates. In the case of SAM-dependent methyl transferases, the degradation of potentially inhibitory SAH<sup>[42]</sup> by *E. coli* enzymes like SAH-hydrolase or methylthioadenosine nucleosidase could also be beneficial. In addition, the time course experiments showed that the reactions with the MBP-JerF-containing cell-free lysate were faster and more complete than those with the purified enzyme, without compromising the products' ee (Figures S76 and S77). The precursors *rac*-21 a–*rac*-21 c were reacted under these conditions on the 100 μmol scale and the efficient isolation of the products was supported by pre-extraction treatment with proteinase, which limits inclusion in the protein precipitate.<sup>[41]</sup> Significantly higher yields than in the 20 μmol scale assays and for *rac*-21 a and *rac*-21 c also significantly higher conversions than on the 2 μmol scale assays were observed (Table 1, column '100 μmol scale').

To further improve the efficiency and the outcome of the biocatalytic reactions, we implemented a HMT-based SAM regeneration system.<sup>[16,43]</sup> The HMT from the thiopurine methyltransferase (TPMT) superfamily isolated from *Ustilago maydis* (*uma*) was chosen, because it has shown the flexibility to also regenerate SAM derivatives such as SAE, which is useful for future applications.<sup>[15,44]</sup> When the *uma*-HMT was integrated into the established reaction of JerF with *rac*-21 a–*rac*-21 c, the conversions and yields were again higher than in the case without (Table 1, column '100 μmol scale + SAM regeneration'). A possible reason for this result could be that the inhibition of JerF by SAH was significantly reduced due to its constant re-methylation to SAM by the *uma*-HMT.<sup>[42]</sup> A spontaneous O or C methylation by Mel did not occur when the MBP-JerF lysate was omitted from the reaction.

As part of the study, a system consisting of an MAT for the in situ formation of SAM from stoichiometric amounts of methionine and ATP and the MTAN from *E. coli* was also tested with JerF.<sup>[13,14]</sup> In these experiments, protein precipitation occurred frequently, so that good yields could not be reliably achieved and the HMT system was further used. A

particular tendency of MAT and EcMTAN to precipitate has not been described in the literature, so this problem is probably due to the properties of JerF and is consistent with the problems encountered in the production of purified JerF.

### Mutational Studies

To better understand the stereoselectivity of JerF in the O-methylation leading to kavalactones, an AlphaFold 2 (AF2)-based structural model was generated in which the cofactor SAM and the two enantiomers of **21 a** were integrated by docking simulations (Figure 4). The structural model exhibited typical features of a type I MT<sup>[45]</sup> such as a Rossmann-fold bearing seven  $\beta$ -strands connected by  $\alpha$ -helices as well as a glycine-rich loop region (residues 57 to 63) and a highly conserved acidic residue (aspartate 81) that interacts with the ribose moiety of SAM. The predicted substrate binding site was exposed on the surface of the protein, consistent with the observed substrate promiscuity. Pronounced differences in the binding and spatial orientation of the two precursor stereoisomers (*R*)-**21 a** and (*S*)-**21 a** in the active site were not immediately apparent.

Three amino acids within 5 Å of the putative substrate-binding site were identified as likely to contribute critical interactions with the substrate based on empirical considerations. F25 could develop  $\pi$ - $\pi$  interactions with the aromatic ring of the substrates. R18 could be a suitable base to facilitate deprotonation of the substrate to accelerate its methylation. Y22 is a candidate for enantiomer-specific interactions at the site of O-methylation and is therefore potentially important in explaining the discrimination between (*R*)-**21 a** and (*S*)-**21 a**. Four specific point mutants at these positions were generated using a modified Quick Change™ protocol and the performance of the resulting

mutant enzymes in the reaction with *rac*-**21 a** was compared to the wild type. Phenylalanine at position 25 was mutated to the similar tyrosine and the significantly smaller alanine. Consistent with the importance of this position, the F25Y mutant already showed a significant decrease in conversion with increased enantioselectivity. The F25A mutant showed a result very different from the wild type, producing a dominant non-isolatable by-product (Figure S121). Mutation of Y22 into the somewhat less voluminous and more polar heteroaromatic histidine led to an almost complete loss of methylation activity, also suggesting crucial interactions of this amino acid with the substrate. Substituting R18 by the smaller and significantly less basic histidine had little effect on conversion and enantioselectivity pointing towards little contribution of this residue to the binding and conversion of the substrate.

These results suggest that Y22 and F25 in the active site of JerF are residues that could be considered for further optimization of the enzyme's performance by engineering. Increasing the ability of JerF to discriminate between precursor enantiomers could be essential to improve the described chemoenzymatic dynamic kinetic resolution process (Scheme 1). A crystal structure of JerF has not yet been obtained but would provide an optimal basis for this type of study in the future.

### Conclusions

This study presents the soluble production of the O-methyltransferase JerF from *jerangolid* biosynthesis, which was previously inaccessible in isolated form, as a purified N-terminal MBP-tagged fusion protein as well as its biochemical characterization. The kinetic parameters were determined with its natural substrate *projerangolid* (**1**) and the enantiom-

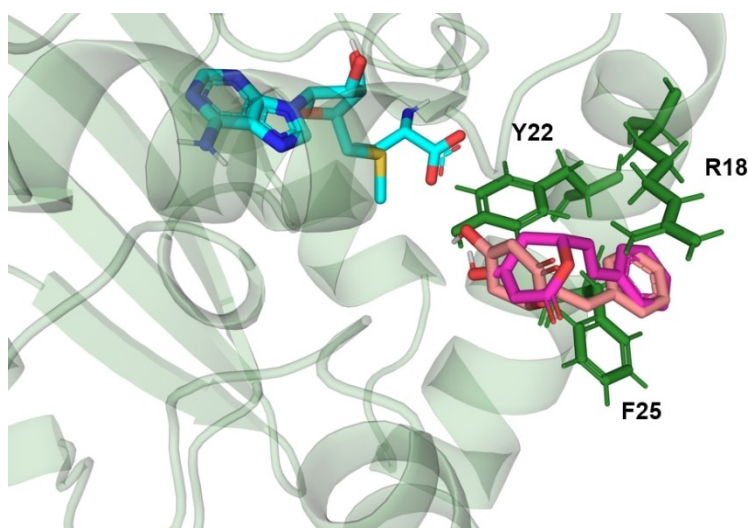


**Figure 4.** AF2-based structural model of JerF with the cofactor SAM (cyan carbons), (*R*)-**21** (magenta carbons) and (*S*)-**21** (light pink carbons) docked in the active site.: Likely substrate binding pocket with residues selected for mutational studies highlighted in dark green. The conversion and *ee* values for the reaction of *rac*-**21 a** with wild-type JerF and the specified mutants are listed in the table. Data was obtained as described for Table 1 [a] see Figure S121 for further information. n.d.: not determined.

mutation	conversion	ee
WT	46	76
F25A	different product <sup>[a]</sup>	n.d.
F25Y	21	86
Y22H	5	n.d.
R18H	44	80

ers of the Ph-derivative **21 a**. A preference of MBP-JerF for (*R*)-**21 a** over (*S*)-**21 a** that had been observed in bioconversions with *jerF\_E. coli* before was confirmed. Together with a spontaneous racemization of ketolactones of the type of **21** occurring at pH 7.4, a dynamic kinetic resolution was obtained, allowing a new chemoenzymatic approach for the synthesis of (+)-kavalactone-like compounds. This was used for the synthesis of the natural products (+)-kavain ((*R*)-**7 a**) and (+)-methysticin ((*R*)-**7 d**/(*R*)-**10**), the known synthetic derivative (+)-11,12-dimethoxykavain ((*R*)-**7 b**)<sup>[28]</sup> as well as the new compounds (+)-12-fluorokavain ((*R*)-**7 c**), and (*R*)-**7 e**. Optimization of the reaction protocol and combination with an HMT-based SAM regeneration system enabled the synthesis of compounds (*R*)-**7 a**-(*R*)-**7 c** on a 100 μmol scale starting from readily available starting materials with overall yields of 37–57% over 3–4 steps and *ees* of 70–86%. A mutational study based on an AlphaFold 2 model of JerF provided initial insights into active site residues potentially involved in the stereodifferentiation. These could be targets for detailed protein engineering studies in the future to better adapt the enzyme to kavalactone-like precursors, in particular by accelerating substrate turnover and enantiomeric specificity.

## Supporting Information Summary

The authors have cited additional references within the Supporting Information.<sup>[28,46–52]</sup>

## Acknowledgements

We thank the Northern Bavarian NMR Centre and the Central Analytics of the Department of Chemistry for analytical measurements. We thank Prof. Florian Seebeck (University of Basel) for providing *pET28-a(+)\_uma*, Dr. Gunter Stier (EMBL, Heidelberg) for providing the pETMBP-1a expression plasmid and Prof. Jennifer Andexer for helpful discussions. We gratefully acknowledge funding from the FP7 People Program of the European Union (293430) and the Deutsche Forschungsgemeinschaft (grant numbers HA 5841/2-1 and HA 5841/7-1). Open Access funding enabled and organized by Projekt DEAL.

## Conflict of Interests

The authors declare no conflict of interest.

## Data Availability Statement

The data that support the findings of this study are available in the supplementary material of this article.

**Keywords:** Methyltransferases · Kavalactones · Chemoenzymatic synthesis · Natural products · Biocatalysis

- [1] J. Li, A. Amatuni, H. Renata, *Curr. Opin. Chem. Biol.* **2020**, *55*, 111–118.
- [2] S. Friedrich, F. Hahn, *Tetrahedron* **2015**, *71*, 1473–1508.
- [3] K. L. Dunbar, D. H. Scharf, A. Litomska, C. Hertweck, *Chem. Rev.* **2017**, *117*, 5521–5577.
- [4] M. R. Bennett, S. A. Shepherd, V. A. Cronin, J. Micklefield, *Curr. Opin. Chem. Biol.* **2017**, *37*, 97–106.
- [5] E. Abdelraheem, B. Thair, R. F. Varela, E. Jockmann, D. Popadić, H. C. Hailes, J. M. Ward, A. M. Iribarren, E. S. Lewkowicz, J. N. Andexer, P.-L. Hagedoorn, U. Hanefeld, *ChemBioChem* **2022**, *23*, e202200212.
- [6] P. de S. M. Pinheiro, L. S. Franco, C. A. M. Fraga, *Pharmaceuticals* **2023**, *16*, 1157.
- [7] E. Romero, B. S. Jones, B. N. Hogg, A. Rué Casamajo, M. A. Hayes, S. L. Flitsch, N. J. Turner, C. Schnepel, *Angew. Chem. Int. Ed.* **2021**, *60*, 16824–16855.
- [8] C. Zhang, S. A. Sultan, R. T. X. Chen, *Bioresour. Bioprocess.* **2021**, *8*, 72.
- [9] P. Germer, J. N. Andexer, M. Müller, *Synthesis* **2022**, *54*, 4401–4425.
- [10] F. Michailidou, A. Rentmeister, *Org. Biomol. Chem.* **2021**, *19*, 3756–3762.
- [11] C. Liao, F. P. Seebeck, *Nat. Catal.* **2019**, *2*, 696–701.
- [12] S. Singh, J. Zhang, T. D. Huber, M. Sunkara, K. Hurley, R. D. Goff, G. Wang, W. Zhang, C. Liu, J. Rohr, S. G. Van Lanen, A. J. Morris, J. S. Thorson, *Angew. Chem. Int. Ed.* **2014**, *126*, 4046–4050.
- [13] F. Subrizi, Y. Wang, B. Thair, D. Méndez-Sánchez, R. Roddan, M. Cárdenas-Fernández, J. Siegrist, M. Richter, J. N. Andexer, J. M. Ward, H. C. Hailes, *Angew. Chem. Int. Ed.* **2021**, *60*, 18673–18679.
- [14] J. Siegrist, S. Aschwanden, S. Mordhorst, L. Thöny-Meyer, M. Richter, J. N. Andexer, *ChemBioChem* **2015**, *16*, 2576–2579.
- [15] K. H. Schülke, F. Ospina, K. Hörschemeyer, S. Gergel, S. C. Hammer, *ChemBioChem* **2022**, *23*, e202100632.
- [16] S. Mordhorst, J. Siegrist, M. Müller, M. Richter, J. N. Andexer, *Angew. Chem. Int. Ed.* **2017**, *56*, 4037–4041.
- [17] F. Ospina, K. H. Schülke, J. Soler, A. Klein, B. Prosenc, M. Garcia-Borràs, S. C. Hammer, *Angew. Chem. Int. Ed.* **2022**, *61*, e202213056.
- [18] L. L. Bengel, B. Aberle, A.-N. Egler-Kemmerer, S. Kienzle, B. Hauer, S. C. Hammer, *Angew. Chem. Int. Ed.* **2021**, *60*, 5554–5560.
- [19] F. Hahn, F. M. Guth, *Nat. Prod. Rep.* **2020**, *37*, 1300–1315.
- [20] B. Julien, Z.-Q. Tian, R. Reid, C. D. Reeves, *Chem. Biol.* **2006**, *13*, 1277–1286.
- [21] F. Hemmerling, K. E. Lebe, J. Wunderlich, F. Hahn, *ChemBioChem* **2018**, *19*, 1006–1011.
- [22] F. M. Guth, F. Lindner, S. Ryzdek, A. Peil, S. Friedrich, B. Hauer, F. Hahn, *ACS Chem. Biol.* **2023**, *18*, 2450–2456.
- [23] F. Lindner, S. Friedrich, F. Hahn, *J. Org. Chem.* **2018**, *83*, 14091–14101.
- [24] S. Friedrich, F. Hemmerling, F. Lindner, A. Warnke, J. Wunderlich, G. Berkhan, F. Hahn, *Molecules* **2016**, *21*, 1443.
- [25] M. Müller, J. He, C. Hertweck, *ChemBioChem* **2006**, *7*, 37–39.
- [26] J. Piel, C. Hertweck, P. R. Shipley, D. M. Hunt, M. S. Newman, B. S. Moore, *Chem. Biol.* **2000**, *7*, 943–955.
- [27] T. F. Schäberle, *Beilstein J. Org. Chem.* **2016**, *12*, 571–588.
- [28] S. Hati, Q. Hu, Z. Huo, J. Lu, C. Xing, *ChemMedChem* **2022**, *17*, e202100727.
- [29] M. H. Pittler, E. Ernst, *J. Clinical. Psychopharmacol.* **2000**, *20*, 84.
- [30] A. Volgin, L. Yang, T. Amstislavskaya, K. Demin, D. Wang, D. Yan, J. Wang, M. Wang, E. Alpyshov, G. Hu, N. Serikuly, V. Shevyrin, E. Wappler-Guzzetta, M. De Abreu, A. Kalueff, *ACS Chem. Neurosci.* **2020**, *11*, 3893–3904.
- [31] T. E. Smith, M. Djang, A. J. Velander, C. W. Downey, K. A. Carroll, S. Van Alphen, *Org. Lett.* **2004**, *6*, 2317–2320.
- [32] P. A. Amaral, N. Gouault, M. L. Roch, V. L. Eifler-Lima, M. David, *Tet. Lett.* **2008**, *49*, 6607–6609.
- [33] A. V. Moro, F. S. P. Cardoso, C. R. D. Correia, *Org. Lett.* **2009**, *11*, 3642–3645.
- [34] G. Sabitha, K. Sudhakar, J. S. Yadav, *Tet. Lett.* **2006**, *47*, 8599–8602.
- [35] A. A. Shaik, J. Tan, J. Lü, C. Xing, *Arkivoc* **2012**, *2012*, 137–145.
- [36] D. Kostermans, *Nature* **1950**, *166*, 788–789.
- [37] P. Schneider, B. Henßen, B. Paschold, B. P. Chapple, M. Schatton, F. P. Seebeck, T. Classen, J. Pietruszka, *Angew. Chem. Int. Ed.* **2021**, *60*, 23412–23418.
- [38] J. Xiao, Q. Zhang, Y. Zhu, S. Li, G. Zhang, H. Zhang, K. Saurav, C. Zhang, *Appl. Microbiol. Biotechnol.* **2013**, *97*, 9043–9053.
- [39] F. Li, L. Yang, J. Zhang, J. S. Chen, H. Renata, *Angew. Chem. Int. Ed.* **2021**, *133*, 17821–17826.

- [40] R. Li, H. J. Wijma, L. Song, Y. Cui, M. Otzen, Y. Tian, J. Du, T. Li, D. Niu, Y. Chen, J. Feng, J. Han, H. Chen, Y. Tao, D. B. Janssen, B. Wu, *Nat. Chem. Biol.* **2018**, *14*, 664–670.
- [41] T. Hollmann, G. Berkhan, L. Wagner, K. H. Sung, S. Kolb, H. Geise, F. Hahn, *ACS Catal.* **2020**, *10*, 4973–4982.
- [42] V. M. Richon, D. Johnston, C. J. Sneeringer, L. Jin, C. R. Majer, K. Elliston, L. F. Jerva, M. P. Scott, R. A. Copeland, *Chem. Biol. Drug Des.* **2011**, *78*, 199–210.
- [43] C. Liao, F. P. Seebeck, *Angew. Chem. Int. Ed.* **2020**, *59*, 7184–7187.
- [44] X. Wen, F. Leisinger, V. Leopold, F. P. Seebeck, *Angew. Chem. Int. Ed.* **2022**, *61*, e202208746.
- [45] Q. Sun, M. Huang, Y. Wei, *Acta Pharmaceut. Sin. B* **2021**, *11*, 632–650.
- [46] S. Sarker, J. Armstrong, P. G. Waterman, *Phytochem.* **1995**, *40*, 1159–1162.
- [47] J. I. Bowen, L. Wang, M. P. Crump, C. L. Willis, *Org. Biomol. Chem.* **2021**, *19*, 6210–6215.
- [48] X. Gan, Z. Fu, L. Liu, Y. Yan, C. Chen, Y. Zhou, J. Dong, *Tet. Lett.* **2019**, *60*, 150906.
- [49] P. S.-W. Leung, Y. Teng, P. H. Toy, *Org. Lett.* **2010**, *12*, 4996–4999.
- [50] G. Battistuzzi, S. Cacchi, G. Fabrizi, *Org. Lett.* **2003**, *5*, 777–780.
- [51] J. Bogomolovas, B. Simon, M. Sattler, G. Stier, *Prot. Express. Purif.* **2009**, *64*, 16–23.
- [52] H. Liu, J. H. Naismith, *BMC Biotechnol.* **2008**, *8*, 91.

---

Manuscript received: May 16, 2024

Revised manuscript received: August 23, 2024

Accepted manuscript online: August 26, 2024

Version of record online: October 24, 2024